

A calculation of the time-of-flight distribution of trapped atoms

I. Yavin, M. Weel, A. Andreyuk, and A. Kumarakrishnan

Citation: [American Journal of Physics](#) **70**, 149 (2002); doi: 10.1119/1.1424266

View online: <https://doi.org/10.1119/1.1424266>

View Table of Contents: <https://aapt.scitation.org/toc/ajp/70/2>

Published by the [American Association of Physics Teachers](#)

ARTICLES YOU MAY BE INTERESTED IN

[Student understanding of the first law of thermodynamics: Relating work to the adiabatic compression of an ideal gas](#)

[American Journal of Physics](#) **70**, 137 (2002); <https://doi.org/10.1119/1.1417532>

[Measurement of temperature of laser cooled atoms by one-dimensional expansion in a magneto-optical trap](#)

[Review of Scientific Instruments](#) **79**, 013101 (2008); <https://doi.org/10.1063/1.2827517>

[An introduction to Pound–Drever–Hall laser frequency stabilization](#)

[American Journal of Physics](#) **69**, 79 (2001); <https://doi.org/10.1119/1.1286663>

[Doppler-free saturated absorption: Laser spectroscopy](#)

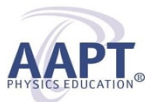
[American Journal of Physics](#) **64**, 1432 (1996); <https://doi.org/10.1119/1.18457>

[Perturbation of infinite networks of resistors](#)

[American Journal of Physics](#) **70**, 153 (2002); <https://doi.org/10.1119/1.1419104>

[High data-rate atom interferometer for measuring acceleration](#)

[Applied Physics Letters](#) **100**, 011106 (2012); <https://doi.org/10.1063/1.3673845>



Advance your teaching and career
as a member of **AAPT**

LEARN MORE



A calculation of the time-of-flight distribution of trapped atoms

I. Yavin, M. Weel, A. Andreyuk, and A. Kumarakrishnan^{a)}

Department of Physics and Astronomy, York University, Toronto M3J 1P3, Canada

(Received 30 July 2001; accepted 4 October 2001)

We consider the ballistic expansion of a cloud of trapped atoms falling under the influence of gravity. Using a simple coordinate transformation, we derive an analytical expression for the time-of-flight signal. The properties of the signal can be used to infer the initial temperature of the cloud. We first assume a point size cloud with an isotropic velocity distribution to explain the physical basis of the calculation. The treatment is then generalized to include a finite-size cloud with an anisotropic velocity distribution, and an exact result for the signal is derived. The properties of the signal are discussed, and an intuitive picture is presented to explain how initial conditions determine the features of the signal. © 2002 American Association of Physics Teachers. [DOI: 10.1119/1.1424266]

I. INTRODUCTION

During the last 15 years, laser cooling and trapping of atoms has become an active area of research. It is now routinely possible to obtain samples of cold atoms with temperatures of $\sim 100 \mu\text{K}$.^{1,2} A measurement of the initial temperature of the cloud of atoms is crucial for characterizing the properties of atom traps. The temperature of the cloud can be inferred from the velocity distribution of atoms in the cloud. A well-known technique of measuring this velocity distribution is the time-of-flight (TOF) method. In this method, a probe laser, focused in the form of a sheet, is placed underneath the cloud (see Fig. 1). When the trapping forces are turned off, the cold atom cloud expands ballistically and falls through the probe under the influence of gravity. It is then possible to detect the fluorescence from the atoms as they reach the sheet. The initial temperature can be inferred by measuring the fluorescence as a function of time.^{3,4}

In this paper we present a detailed derivation of the TOF signal recorded by the detector, that is, the number of atoms arriving at the probe laser as a function of time. We model the laser placed underneath the atom cloud as a plane sheet. We assume that the cloud consists of noninteracting particles and that it has a Maxwell-Boltzmann velocity distribution. We therefore use the equations of ballistic motion for particles falling under the influence of gravity to find their distribution in time and position on the sheet. We then integrate over the spatial dimensions of the probe laser (sheet) to obtain the distribution in time. Previous calculations of the TOF signal have used sophisticated Green's function techniques to find the evolution of the density of the cloud.⁴ Here, we show that the problem can be solved using a simple coordinate transformation, which makes the solution more transparent.

In Sec. II an intuitive description of the solution to the problem is given. For a simplified derivation of the TOF signal, we start in Sec. III with the following two assumptions. (a) We assume a point-sized cloud, that is, we do not consider the spatial extent of the cloud. This assumption is valid if the distance of the probe laser from the cloud is much larger than the size of the cloud. (b) The velocity distribution is isotropic. Subsequently, in Sec. IV, we consider a more realistic model that assumes the cloud has a finite size. In addition, the effect of an anisotropic velocity distribution is investigated in Sec. V.

II. INTUITIVE PICTURE

We first describe the solution to the problem based on simple physical considerations. The initial velocity distribution of the atoms in the cloud is a Gaussian (Maxwell-Boltzmann velocity distribution). It is characterized by the most probable speed $v_0 = \sqrt{2kT/m}$, where k is Boltzmann's constant, T is the initial temperature of the cloud, and m is the atomic mass. The width of the TOF signal should correspond to the difference in arrival times of two atoms, each having the most probable speed v_0 , one going directly upward, and the other directly downward. If the initial density of the cloud is a maximum at the center, then the centroid of the cloud will reach the probe at $t = \sqrt{2l_0/g}$. This time will correspond to a peak in the TOF signal. Here l_0 is the distance from the probe and $g = 9.81 \text{ m/s}^2$ is the earth's gravitational acceleration. Based on the essential features of the TOF signal discussed above, one can expect that its shape will be a Gaussian. We will now proceed to formulate a mathematical treatment of this problem and arrive at an exact solution.

III. CALCULATION FOR A POINT-SIZED ISOTROPIC CLOUD

We assume a Maxwell-Boltzmann isotropic probability distribution for the velocity, that is,

$$N(v)d^3v = \left(\frac{m}{2\pi kT}\right)^{3/2} \exp\left(-\frac{m(v_x^2 + v_y^2 + v_z^2)}{2kT}\right) d^3v, \quad (1)$$

where v_x , v_y , v_z are the speeds along the x , y , z directions in the cloud's coordinate system, respectively. We take the origin of the coordinates to be the initial location of the atom cloud. A second coordinate system is needed to specify the location of the atoms arriving at the sheet at a time t . For this coordinate system we will take the sheet to be the x - y plane with its origin at the point on the sheet just underneath the cloud's center. We need this coordinate system because it represents the measuring apparatus, that is, the probe laser. The problem is therefore reduced to transforming Eq. (1) from a function of (v_x, v_y, v_z) to a function of (x, y, t) .

We use Newton's equations for a ballistic motion of a particle accelerated by the earth's gravitational field to find the relationship between those two coordinates systems,

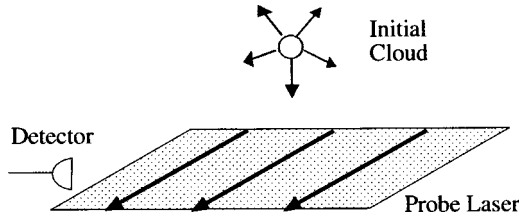


Fig. 1. In a typical experiment, the detector images the fluorescence at a right angle with respect to the direction of propagation of the probe laser beam indicated by the arrows.

$$-l_0 = v_z t - \frac{1}{2} g t^2, \quad (2a)$$

$$x = v_x t, \quad (2b)$$

$$y = v_y t, \quad (2c)$$

where l_0 is the distance from the center of the cloud to the sheet. If we express the velocity components as functions of (x, y, t) , we find

$$v_z = (\frac{1}{2} g t^2 - l_0)/t, \quad (3a)$$

$$v_x = x/t, \quad (3b)$$

$$v_y = y/t. \quad (3c)$$

We must also determine how the differential d^3v in (1) transforms into $dx dy dt$. We use the Jacobian determinant J for this purpose, that is, with

$$J = \begin{vmatrix} \frac{\partial v_x}{\partial x} & \frac{\partial v_x}{\partial y} & \frac{\partial v_x}{\partial t} \\ \frac{\partial v_y}{\partial x} & \frac{\partial v_y}{\partial y} & \frac{\partial v_y}{\partial t} \\ \frac{\partial v_z}{\partial x} & \frac{\partial v_z}{\partial y} & \frac{\partial v_z}{\partial t} \end{vmatrix} = \begin{vmatrix} \frac{1}{t} & 0 & \frac{-x}{t^2} \\ 0 & 1 & \frac{-y}{t^2} \\ 0 & 0 & \frac{1}{2} g + \frac{l_0}{t^2} \end{vmatrix} = \frac{\frac{1}{2} g t^2 + l_0}{t^4}. \quad (4)$$

Substituting Eqs. (3) and (4) into Eq. (1), we find the probability density with respect to the (x, y, t) coordinate system,

$$N(x, y, t) dx dy dt = A \exp\left(-\frac{(\frac{1}{2} g t^2 - l_0)^2 + x^2 + y^2}{v_0^2 t^2}\right) \times \frac{(\frac{1}{2} g t^2 + l_0)}{t^4} dx dy dt. \quad (5)$$

Here, $A = (m/2\pi kT)^{3/2}$ and $v_0 = \sqrt{2kT/m}$ is the most probable velocity.

However, we are interested in the signal recorded, that is, the probability density as a function of time only. We therefore integrate Eq. (5) over the spatial dimensions of the probe. For convenience, we assume the dimensions to be infinite. (To model an experiment, we must perform the integral over a finite region, which would require the integral to be evaluated numerically.) Thus,

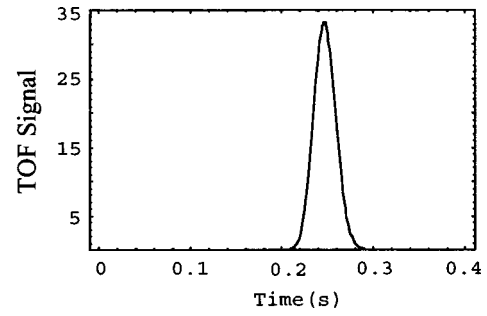


Fig. 2. Time-of-flight (TOF) signal for a point-sized cloud with $T = 1.41 \times 10^{-4}$ K, $l_0 = 0.3$ m, and $m = 1.40 \times 10^{-25}$ kg.

$$n(t) = \int_{-\infty}^{\infty} \int_{-\infty}^{\infty} N(x, y, t) dx dy = A \pi v_0^2 \left(\frac{\frac{1}{2} g t^2 + l_0}{t^2} \right) \exp\left(-\frac{(\frac{1}{2} g t^2 - l_0)^2}{v_0^2 t^2}\right). \quad (6)$$

Figure 2 is a plot of this function with $T = 1.41 \times 10^{-4}$ K (Doppler limit for cloud of ^{85}Rb atoms), $l_0 = 0.3$ m, and $m = 1.40 \times 10^{-25}$ kg (^{85}Rb atoms). A peak occurs at $t = 0.247$ s as one would expect physically, because the centroid of the cloud reaches the detector after $t = \sqrt{2l_0/g} = 0.247$ s.

As described earlier, the width of the signal should correspond to the difference in arrival times between an atom going directly up with speed v_0 and one that goes directly down with the same speed. Using Eq. (2a), this difference is equal to $t_+ - t_- = 2v_0/g$, where

$$t_{\pm} = \frac{\pm v_0 + \sqrt{v_0^2 + 2l_0g}}{g}.$$

Table I shows different temperatures and the corresponding values of the $1/e$ width of the TOF signal calculated using Eq. (6). The width is then compared with $2v_0/g$. We note that the agreement between the two predictions is excellent. The agreement corresponds to our physical expectations as described in Sec. II and serves as a test of Eq. (6). One should note that the difference between the two predictions increases as the temperature (defined by v_0) increases. This difference is due to the fact that the shape of the TOF signal deviates from a Gaussian as discussed at the end of Sec. IV.

Table I. Comparison between the predicted signal width and $2v_0/g$, for different initial temperatures of the cloud. The full width at half maximum (FWHM) is the predicted width of the Gaussian curve at half of its peak value.

Temperature (K)	v_0 (m/s)	$2v_0/g$ (s)	Signal FWHM (s)
1.41×10^{-5}	0.052 723	0.010 760	0.010 759
5.00×10^{-5}	0.099 283	0.020 262	0.020 253
8.50×10^{-5}	0.129 449	0.026 418	0.026 399
1.41×10^{-4}	0.166 725	0.034 025	0.033 985
4.50×10^{-4}	0.297 849	0.060 786	0.060 554
7.50×10^{-4}	0.384 522	0.078 474	0.077 971
1.10×10^{-3}	0.465 679	0.095 037	0.094 135
4.80×10^{-3}	0.972 772	0.198 525	0.189 655

IV. FINITE-SIZE ISOTROPIC CLOUD

We now refine the model by taking into account the spatial extent of the cloud, which we will assume to have a Gaussian shape. The probability density, given by Eq. (1), will now be a function of \mathbf{r} and \mathbf{v} , and is given by

$$N(\mathbf{r}, \mathbf{v}) d^3 r d^3 v = A \exp\left(-\frac{v_x^2 + v_y^2 + v_z^2}{v_0^2}\right) \frac{1}{r_0^3 \pi^{3/2}} \times \exp\left(-\frac{r_x^2 + r_y^2 + r_z^2}{r_0^2}\right) d^3 r d^3 v, \quad (7)$$

where A and v_0 were defined previously, and r_0 is the most probable radial distance. We take the origin of our coordinates (r_x, r_y, r_z) to be the center of the cloud. Following the same route as in Sec. III, we transform this probability density into a function of (\mathbf{r}, x, y, t) using the equations of motion in (2). These equations are modified to include the fact that the initial position of the particle is at \mathbf{r} , that is, some distance from the center of cloud. Therefore,

$$-l_0 = r_z + v_z t - \frac{1}{2} g t^2, \quad (8a)$$

$$x = r_x + v_x t, \quad (8b)$$

$$y = r_y + v_y t. \quad (8c)$$

Using Eq. (8), we express (v_x, v_y, v_z) as functions of $(x, y, t; \mathbf{r})$. Evaluating the Jacobian we find,

$$J = \frac{(\frac{1}{2} g t^2 + r_z + l_0)}{t^4}. \quad (9)$$

If we substitute J into the probability density (7), we obtain

$$N(\mathbf{r}, x, y, t) d^3 r dx dy dt = A \frac{1}{r_0^3 \pi^{3/2}} \frac{(\frac{1}{2} g t^2 + r_z + l_0)}{t^4} \times \exp(-f) d^3 r dx dy dt, \quad (10a)$$

where the argument of the exponential function is given by

$$f = \left(\left(\frac{1}{v_0^2 t^2} + \frac{1}{r_0^2} \right) r_x^2 - \frac{2x}{v_0^2 t^2} r_x + \frac{x^2}{v_0^2 t^2} \right) + \left(\left(\frac{1}{v_0^2 t^2} + \frac{1}{r_0^2} \right) r_y^2 - \frac{2y}{v_0^2 t^2} r_y + \frac{y^2}{v_0^2 t^2} \right) + \left(\left(\frac{1}{v_0^2 t^2} + \frac{1}{r_0^2} \right) r_z^2 - \frac{2(\frac{1}{2} g t^2 - l_0)}{v_0^2 t^2} r_z + \frac{(\frac{1}{2} g t^2 - l_0)^2}{v_0^2 t^2} \right). \quad (10b)$$

We now integrate Eq. (10) over all space to obtain an expression for the probability density as a function of (x, y, t) , that is,

$$N(x, y, t) = \int_{-\infty}^{\infty} \int_{-\infty}^{\infty} \int_{-\infty}^{\infty} N(\mathbf{r}, x, y, t) d^3 r = A \frac{v_0^3}{t} \frac{1}{(r_0^2 + v_0^2 t^2)^{5/2}} \left(l_0 v_0^2 t^2 + \frac{1}{2} g t^2 (2r_0^2 + v_0^2 t^2) \right) \times \exp\left(-\frac{(x^2 + y^2 + (\frac{1}{2} g t^2 - l_0)^2)}{(r_0^2 + v_0^2 t^2)}\right). \quad (11)$$

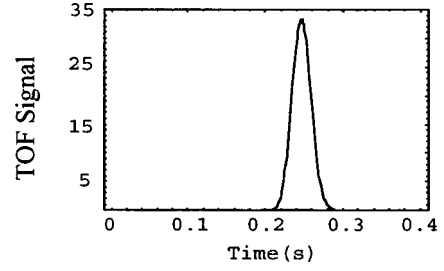


Fig. 3. TOF signal for a finite-size cloud when $r_0 \ll l_0$ with $T = 1.41 \times 10^{-4}$ K, $l_0 = 0.3$ m, $m = 1.40 \times 10^{-25}$ kg, and $r_0 = 0.001$ m.

Again, the signal of interest is obtained by integrating Eq. (11) over the spatial dimensions of the probe laser. We therefore obtain

$$n(t) = \int_{-\infty}^{\infty} \int_{-\infty}^{\infty} N(x, y, t) dx dy = A \frac{v_0^3}{t} \frac{\pi}{(r_0^2 + v_0^2 t^2)^{3/2}} \left(l_0 v_0^2 t^2 + \frac{1}{2} g t^2 (2r_0^2 + v_0^2 t^2) \right) \times \exp\left(-\frac{(\frac{1}{2} g t^2 - l_0)^2}{(r_0^2 + v_0^2 t^2)}\right). \quad (12)$$

Equation (12) reduces to Eq. (6) when $r_0 \rightarrow 0$, as it should for the case of a point size cloud.

Figure 3 is a plot of Eq. (12) with the same parameters as in Fig. 2. We assume $r_0 = 0.001$ m (typical cloud size) and as expected, we obtain the same graph as in Fig. 2 because $r_0 \ll l_0$. However, as r_0 becomes comparable to l_0 , the signal becomes broader and asymmetric as shown in Fig. 4, where we have assumed $r_0 = 0.15$ m. The broadening occurs because we now have many more atoms starting close to the probe. Hence, it takes them less time to reach it. We also have many more atoms that are further away from the probe. Therefore, they will require more time to arrive at it.

We note that the arrival times of two oppositely directed atoms along the vertical, given by

$$t_{\pm} = \frac{\pm v_0 + \sqrt{v_0^2 + 2l_0 g + 2r_0 g}}{g},$$

are asymmetric with respect to the peak of the signal (which occurs at $t = \sqrt{2l_0/g}$). This asymmetry causes the TOF signal shape to deviate from a Gaussian. When the cloud size is small ($r_0 \ll l_0$) and its temperature, that is, the characteristic speed, is low ($v_0^2 \ll 2gl_0$), the arrival times can be written as

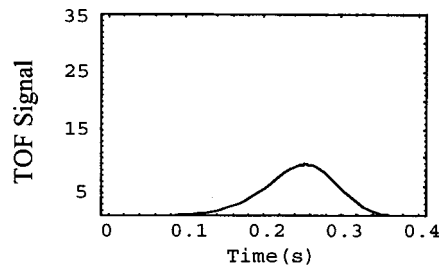


Fig. 4. TOF signal for a finite-size cloud when r_0 is comparable to l_0 with $T = 1.41 \times 10^{-4}$ K; $l_0 = 0.3$ m, $m = 1.40 \times 10^{-25}$ kg, and $r_0 = 0.15$ m.

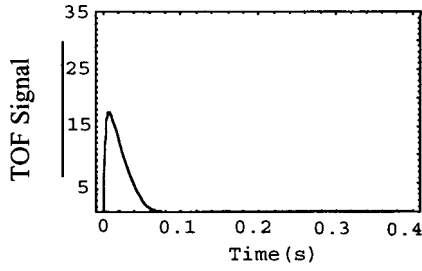


Fig. 5. TOF signal for a finite-size cloud when the probe is placed at the center of the cloud with $l_0=0$; $T=1.41 \times 10^{-4}$ K, $m=1.40 \times 10^{-25}$ kg, and $r_0=0.001$ m.

$$t_{\pm} = \sqrt{\frac{2l_0}{g}} \pm \frac{v_0}{g},$$

which is symmetric about the peak of the signal. For this reason, the signal is symmetric at low temperatures and small cloud dimensions.

Note that the typical size of cold atom clouds never exceeds a few millimeters, and the probe is typically placed at a distance larger than the size of the trapping beams (~ 1 cm). In practice, there is no contribution from the tail of the Gaussian spatial distribution at the location of the probe (there are no cold atoms beyond a few millimeters from the center of the trap).

Figure 5 is a plot of the signal when the probe laser is placed at the center of the cloud (that is, $l_0=0$). We notice the exponential decay of the signal corresponding to atoms leaving the trapping volume. We have also tested the calculation by placing the probe laser above the trap (for example, $l_0 = -2$ mm). In this case we find that the amplitude of the signal is substantially diminished. The reduction in signal amplitude is due to the fact that most of the atoms are turned around by gravity and never reach the probe.

V. ANISOTROPIC FINITE SIZE CLOUD

We now examine the case where the initial temperature of the atom cloud is not necessarily the same in all directions. In this case, one must modify the Maxwell-Boltzmann velocity distribution appropriately,

$$N(\mathbf{r}, \mathbf{v}) d^3 r d^3 v = A \exp\left(-\frac{v_x^2}{v_1^2} - \frac{v_y^2}{v_2^2} - \frac{v_z^2}{v_3^2}\right) \frac{1}{r_0^3 \pi^{3/2}} \times \exp\left(-\frac{r_x^2 + r_y^2 + r_z^2}{r_0^2}\right) d^3 r d^3 v. \quad (13)$$

Here

$$A = \left(\frac{m}{2\pi k}\right)^{3/2} \frac{1}{\sqrt{T_1 T_2 T_3}}, \quad v_i = \sqrt{\frac{2kT_i}{m}}.$$

Following the same steps as in Sec. IV, we arrive at an analytical expression for the observed signal,

$$n(t) = A \frac{v_1 v_2 v_3}{t} \frac{\pi}{(r_0^2 + v_3^2 t^2)^{3/2}} (l_0 v_3^2 t^2 + \frac{1}{2} g t^2 (2r_0^2 + v_3^2 t^2)) \times \exp\left(-\frac{(\frac{1}{2} g t^2 - l_0)^2}{r_0^2 + v_3^2 t^2}\right). \quad (14)$$

We note that the width of the curve depends only on v_3 , r_0 , and l_0 . It is only the vertical speed (along the z direction) that determines the width of the signal. As was explained previously, the width corresponds to the difference in arrival time between two atoms, one going up, and the other going down, both with speed v_3 . This difference is $2v_3/g$.

VI. CONCLUSIONS

Using a simple coordinate transformation, we were able to derive an expression for the TOF signal recorded by a detector placed some distance below the trapped cloud. This coordinate transformation is based on the ballistic equations of motion for a particle falling in the earth's gravitational field. The probe laser was modeled as an infinite plane sheet. The cloud has a Gaussian spatial profile and a Maxwell-Boltzmann velocity distribution. By fitting an experimental result to the predicted signal, one can determine the initial temperature of the cloud.

We note that our calculations are carried out by assuming that the probe laser is an infinite sheet of negligible thickness. Our results would be in perfect agreement with Ref. 4 (where the TOF signal was derived using Green's function techniques), if the integral in Eq. (12) is evaluated by taking into account the spatial profile of the probe. The discrepancy arises because Ref. 4 assumes an elliptical cross section for the probe beam. As mentioned previously, in order to model an experiment, one has to integrate Eq. (12) over the finite extent of the probe. Finally, we note that the calculation can model a probe laser placed at any location in space, including the region of the trap. Thus the calculation can predict the time it takes atoms to leave the trapping volume.

ACKNOWLEDGMENTS

Support for IY and MW was through undergraduate research scholarships. This research is supported by Canada Foundation for Innovation, Ontario Innovation Trust, York University and National Science and Engineering Research Council of Canada. We would also like to acknowledge helpful comments from Helen Freedhoff of York University.

^aElectronic mail: akumar@yorku.ca

¹E. L. Raab, M. Prentiss, A. Cable, S. Chu, and D. E. Pritchard, "Trapping of neutral sodium atoms with radiation pressure," *Phys. Rev. Lett.* **59**, 2631–2634 (1987).

²C. Monroe, W. Swann, H. Robinson, and C. Wieman, "Very cold trapped atoms in a vapor cell," *Phys. Rev. Lett.* **65**, 1571–1574 (1990).

³P. D. Lett, W. D. Phillips, S. L. Rolston, C. E. Tanner, R. N. Watts, and C. I. Westbrook, "Optical molasses," *J. Opt. Soc. Am. B* **6**, 2084–2107 (1989).

⁴D. S. Weiss, E. Riis, Y. Shevy, P. J. Ungar, and S. Chu, "Optical molasses and multilevel atoms: Experiment," *J. Opt. Soc. Am. B* **6**, 2072–2083 (1989).